

SYNTHESIS OF NEW BORON COMPOUNDS WITH AMOXICILLIN AND SOME OF ITS METAL COMPLEXES WITH USE THEM IN ANTIBACTERIAL, ASSESSMENT OF HEPATOPROTECTIVE AND KIDNEYACTIVITY, ANTICANCER AND ANTIOXIDANT APPLICATIONS

GHANEM SH AL-JEBOURI*, ASMAA MOHAMMED NOORIKHALEEL

Department of Chemistry, College of Sciences, University of Baghdad, Baghdad, Iraq. Email: ghanemshaker93@gmail.com

Received: 22 November 2018, Revised and Accepted: 29 December 2018

ABSTRACT

Objective: New ligand ({7-[2-amino-2-(4-hydroxyphenyl)-acetamido-3,3-dimethyl-6-oxo-2-thia-5-aza bicyclo[3,2,0]heptane-4-carboxylic boric anhydride}) with its Co (II), Ni (II) and Cu (II) complexes. And new mixed ligand copper complex was synthesized.

Methods: The ligand was synthesized by the reaction of boric acid with amoxicillin (1:1) and the mixed ligand complex has been synthesized by the reaction of the ligand, 4-aminoantipyrine and Cu (II) ion (1:1:1).

Results: All studied compounds were characterized by the spectral method: Fourier transform infrared, ultraviolet-visible, thermal analysis (TG and DTG), flame atomic absorption and nuclear magnetic resonance. Also CHNS, melting point, magnetic susceptibility and molar conductivity.

Conclusion: According to the obtained data, all complexes were non electrolyte and the geometry was octahedral for all complexes. All synthesized compounds were tested as antibacterial agents against *Escherichia Coli*, *Pseudomonas auroginosa* as Gram-negative bacteria (G-) and *Staphylococcus aureus epidermis* as Gram-positive bacteria (G+). The results showed that copper complexes were more active in (10-2M) than the other compounds. The medicinal applications (hepatoprotective and kidney in serum of mice, histopathological of liver and kidney, anticancer and antioxidant in human cell were studied of the synthesized compounds and gave a good results in all tested.

Keywords: Boron compounds, Boric acid, Amoxicillin, Anticancer, Antioxidant.

© 2019 The Authors. Published by Innovare Academic Sciences Pvt Ltd. This is an open access article under the CC BY license (<http://creativecommons.org/licenses/by/4.0/>) DOI: <http://dx.doi.org/10.22159/ajpcr.2019.v12i3.30912>

INTRODUCTION

Boric acid and borates are exists in water, food and soil. They are used as least toxic pesticides to kill insects, mites, fungi, algae, fleas and wood decay fungi [1]. The mechanism of killing contains working to poison the stomach and absorbing the waxes which protect insects. Also boric acid used as antiseptic in talcum powder, mouth-washes, eyewashes and protective ointments. Another application includes reducing the flammability of cellulosic materials used in production of leather [2].

Amoxicillin trihydrate (2-Amino-2,3,3-dimethyl-7-oxo-4-thia-1-azabicyclo [3.2.0] heptane-2-carboxylic acid) [3]. The amoxicillin is a widely used in biological and pharmaceutical applications [4]. It is used as respiratory, veterinary medicine to treatment the gastrointestinal, antibiotic in human medicine as well as skin and urinary bacterial infections [5].

4-Aminoantipyrine (4-amino-2,3-dimethyl-1-phenyl-3-pyrazolin-5-one (4-AAP)) [6] is one of aromatic compounds which has a special properties and used as antipyretic, anti-inflammatory, analgesic, antimicrobial and anticancer [6].

In the present work we are synthesis a new derivative of amoxicillin with boric acid, also the metal complexes of this derivative (ligand) with Co (II), Ni (II) and Cu (II) ions were synthesized. We are synthesis a mixed ligand complex from the reaction of amoxicillin and 4-aminoantipyrine with Cu (II) ion. The medicinal applications and the biological activity were studied for all synthesized compounds.

EXPERIMENTAL PART**Chemicals**

All chemicals were used as received without further purification (supplied by BDH, Spain, Aldrich, Merck, FlukaAG, BuchsSG, LOBA Chime, Hayman. Fluka-Garantie and fieser).

METHODS**Synthesis of 7-[2-amino-2-(4-hydroxyphenyl)-acetamido-3,3-dimethyl-6-oxo-2-thia 5-aza bicyclo[3,2,0]heptane-4-carboxylic boric anhydride (L) (Fig. 1)**

The mixture of amoxicillin trihydrate (0.1 g, 0.238 mmol) in 10 mL H₂O and boric acid (0.0147 g, 0.238 mmol) in 1 mL H₂O was heated under reflux for 17 h with stirring. The resulting solution was heated to evaporate part of a solvent and then diethyl ether was added in presence of ice-bath and crushing to precipitate the yellow product, washed with hot water and dried in oven.

Synthesis of metal complexes with Co (II), Ni (II) and Cu (II) (C1-C3)

The mixture of L (0.1 g, 0.244 mmol) in 5 mL methanol and metal salt (0.244 mmol, 0.058, 0.057 and 0.041 g) of CoCl₂·6H₂O, NiCl₂·6H₂O and CuCl₂·2H₂O respectively in 1 mL methanol was heated under reflux for (5) h with stirring. The part of solvent was evaporated and diethyl ether was added in presence of ice-bath and crushing to increase the quantity of product, washed with methanol and dried in oven.

Synthesis of mixed ligand complex with Cu (II) ion (Mix.)

The mixture of L(0.115 g, 0.281 mmol) in 3 mL methanol, 4-aminoantipyrine (0.057 g, 0.281 mmole) in 1 mL methanol and CuCl₂·2H₂O (0.048 g, 0.281 mmole) in 1 mL methanol was heated under reflux for 5 h. Part of solvent was evaporated and diethyl ether was added in presence of ice-bath and crushing to increase the product. The black product washed several time with methanol and dried in oven.

Antibacterial activity

Antibacterial activity of the ligand and its metal complexes was studied against *Pseudomonas auroginosa* and *Escherichia Coli* as Gram-negative (G-) and *S. aureus* as Gram-positive (G+) by the agar well-diffusion

method. The concentration of solutions were 10^{-2} and 10^{-3} M in description dimethyl sulfoxide (DMSO) and incubated at 37°C for 24 h.

The hepatoprotective and kidney effects

The hepatoprotective and kidney effects were evaluation in mice which treated with the ligand (L), Copper complex (C_3) and mixed ligand complex (Mix). This test included liver function test glutamic oxaloacetic transaminase (GOT), glutamate pyruvate transaminase (GPT) and alkaline phosphatase (ALP) and kidney function (Urea, Creatinine, Albumin (Alb), Total serum protein (TSP) test and in serum.

The hepatoprotective test

The commercial kit of GOT, GPT and ALP were (Randox company) method [7,8].

The kidney function test

The commercial kit of urea, creatinine, Alb and TSP were (Agappe company) method [9-11].

Statistical analysis

The values of the investigated parameters were given in terms of mean \pm standard error, by using the computer programmer SPSS version 13.0 [12].

Histopathological study

After blood collection, the mouse was dissected and to obtain the liver and kidney. The histopathological examination was adopted on the litreture [13].

Anticancer and antioxidant activity

The MTT cell viability assay was worked using 96-well plate for determination of cytotoxic effect. The cell lines were seeded at 1×10^4 cells/well. After 24 h, cell were treated with studied compounds. The study of anticancer effectiveness was based on literature [14] and the absorbance was measured at 492 nm.

Antioxidant activity of x-substance was determined using stable DPPH radicals as well as the minor modification [15].

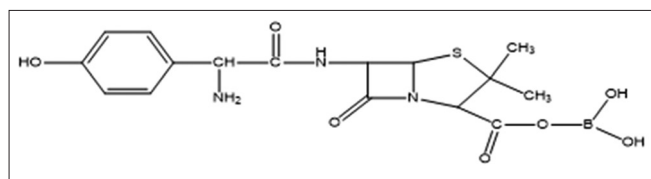


Fig. 1: 7-[2-Amino-2-(4-hydroxyphenyl)-acetamido-3,3-dimethyl-6-oxo-2-thia 5-aza bicyclo[3,2,0]heptane-4-carboxylic boric anhydride (L)

RESULTS AND DISCUSSION

Physical properties and elemental analysis

The physical properties, elemental and analytical data are illustrated in Table 1.

FT-IR Spectroscopy

The FT-IR spectrum of the ligand showed bands at $3456, 3379 \text{ cm}^{-1}$ which refer to stretching vibration of NH_2 [16]. The band of ν N-H (amide) was appeared at 3205 cm^{-1} [16]. The spectrum of exhibited absence of carboxylic OH band ($3300\text{--}2621 \text{ cm}^{-1}$ in amoxicillin) and appear new band at 1342 cm^{-1} , which due to ν O-B [17, 18]. The spectrum showed band at 3525 cm^{-1} which was assigned to phenolic OH group [16]. The band of ν C=O (carboxylic and β -lactam) was appeared at 1770 cm^{-1} [16, 18]. While the band of ν C=O of amide appeared at 1683 cm^{-1} [16]. The data can be shown in Table 2. The spectra of complexes C_1, C_3, Mix . showed shifting in some band positions. The bands of ν NH_2 shifted to higher frequency of asymmetry bands and to lower frequency of symmetric bands (Table 2) and this refer to coordination with metal ions through the nitrogen atom of NH_2 [4]. The band of ν NH (amide) was shifted to higher frequency in all complexes and this is attributed to coordination with metal ions. The spectrum of mixed ligand showed a new band at 1560 cm^{-1} due to imine (ν C=N) [19]. All spectra of complexes exhibited new bands at lower frequency which refer to ν M-O, ν M-N and ν M-Cl [20]. The data can be shown in Table 2.

NMR Spectroscopy

^1H NMR and ^{13}C NMR were used to characterized the ligand (L) and its metal complexes using d_6 -DMSO as solvent.

^1H -NMR Spectroscopy

The spectra of all compounds showed peak at δ 2.5 ppm which refer to chemical shift of DMSO as a solvent. The spectra of exhibited absence the proton peak of carboxylic OH (about δ 10 ppm in amoxicillin) [21] and appear new proton peak of B-OH at δ 8.74 pp [22] (Table 3). The spectra of Co (II), Ni (II) and Cu (II) complexes ($C_1\text{--}C_3$) were showed shifting to higher value in proton peak position of N-H amide and NH_2 groups (Tables 4-6) comparison with the spectrum of ligand (L) [21]. The spectrum of (Mix.) exhibited further proton peaks which attributed to 4-aminoantipyrene [19]. The spectrum of (Mix.) also showed shifting in position of chemical shift of N-H amide and NH_2 comparison with the ligand (Table 7) because the complexation with metal ions through nitrogen atoms of N-H amide and NH_2 . The spectrum of (Mix.) also showed shifting to higher values in position peaks of N-CH and this is because formation of imine group in neighboring atom [21]. The spectra of the ligand and C_3 can be shown in Figs. 2-4.

^{13}C NMR Spectroscopy

The ^{13}C NMR data are listed in (Tables 8-12). The chemical shift of DMSO as a solvent appeared at δ 40 ppm. The ^{13}C NMR spectrum of the ligand (L) showed shifted to higher values of carboxylic C=O group

Table 1: Analytical data and physical properties of the ligand and its metal complexes

Comp.	The molecular formula	Color	m.p ($^{\circ}\text{C}$)	Yield%	M.wt g.mol-	Micro elemental analysis found (Calc.)				Metal content%	Chloride content%
						C%	H%	N%	S%		
L	$\text{C}_{16}\text{H}_{20}\text{N}_3\text{O}_7\text{SB}$	Yellow	182–184	51.54	408.82	46.39 (46.96)	5.2 (4.89)	10.04 (10.27)	7.13 (7.82)	--	--
C1	$\text{C}_{16}\text{H}_{20}\text{N}_3\text{O}_7\text{SBCo}$. 2Cl. $2\text{H}_2\text{O}$	Green	210–212	42.85	574.73	33.21 (33.41)	4.43 (4.18)	7.21 (7.31)	5.48 (5.56)	10.13 (10.25)	12.12 (12.35)
C2	$\text{C}_{16}\text{H}_{20}\text{N}_3\text{O}_7\text{SBNi}$. 2Cl. $2\text{H}_2\text{O}$	Brown	240–242	50.00	574.49	34.33 (33.42)	4.13 (4.20)	7.18 (7.31)	5.64 (5.57)	9.93 (10.21)	12.24 (12.35)
C3	$\text{C}_{16}\text{H}_{20}\text{N}_3\text{O}_7\text{SBCu}$. 2Cl. $2\text{H}_2\text{O}$	Black	140 Dec	57.14	579.366	34.01 (33.14)	4.22 (4.14)	7.44 (7.25)	5.01 (5.52)	10.70 (10.97)	12.05 (12.25)
Mix.	$\text{C}_{27}\text{H}_{31}\text{N}_6\text{O}_7\text{SBCu}$. 2Cl. $2\text{H}_2\text{O}$	Black	228–230	52.08	764.36	42.39 (42.38)	4.32 (4.57)	10.62 (10.98)	4.22 (4.18)	8.12 (8.31)	8.99 (9.28)

Dec: Decompose, M.wt: Molecular weight

Table 2: Characteristic infrared absorption bands of the ligand and its metal complexes

Comp	ν NH2	ν NH amide	ν OH carboxylic. Acid	OH phenolic	ν C=O β -lactam and carboxylic. Acid	ν C=O amide	ν B-O	ν C=N	ν M-O	ν M-N	ν M-Cl
L	3456 3379	3205	-----	3525	1770	1683	1342	-----	-----	-----	-----
C1 (Co)	3471 3350	3232	-----	3527	1730	1645	1345	-----	435	568	389
C2 (Ni)	3482 3355	3235	-----	3533	1750	1652	1346	-----	438	565	362
C3 (Cu)	3483 3355	3251	-----	3529	1733	1654	1340	-----	489	568	360
Mix.	3482 3355	3225	-----	3523	1750	1652	1334	1560	536	449	366

Table 3: ¹HNMR data for the ligand

Assignments in d6-DMSO	Chemical shifts δ (ppm)
OH Phenolic	9.33 (1H), s
B-OH	8.74 (2H), s
N-H Amide	8.64 (1H), s
C-H aromatic	7.37-7.23 (4H), m
CHNH (β -lactam)	5.62 (1H), d
CHS (β -lactam)	5.32 (1H), d
NH ₂	4.98 (2H), s
CH-NH ₂	4.98 (1H), s
N-CH	3.99 (1H), s
2CH ₃	1.49 (3H), s, 1.40 (3H), s

DMSO: Dimethyl sulfoxide

Table 4: ¹HNMR data for C1

Assignments in d6-DMSO	Chemical shifts δ (ppm)
OH Phenolic	9.20 (1H), s
N-H Amide	9.09 (1H), s
B-OH	8.83 (2H), s
C-H aromatic	8.03-6.50 (4H), m
CHNH (β -lactam)	5.69 (1H), d
CHS (β -lactam)	5.42 (1H), d
NH ₂	5.29 (2H), s
CH-NH ₂	5.29 (1H), s
N-CH	3.96 (1H), s
H ₂ O	3.57 (4H), s
2CH ₃	1.29 (3H), s, 1.16 (3H), s

DMSO: Dimethyl sulfoxide

Table 5: ¹HNMR data for C2

Assignments in d6-DMSO	Chemical shifts δ (ppm)
OH Phenolic	9.26 (1H), s
N-H Amide	8.99 (1H), s
B-OH	8.85 (2H), s
C-H aromatic	8.02 - 6.50 (4H), m
CHNH (β -lactam)	5.70 (1H), d
CHS (β -lactam)	5.47 (1H), d
NH ₂	5.32 (2H), s
CH-NH ₂	5.32 (1H), s
N-CH	3.99 (1H), s
H ₂ O	3.43 (4H), s
2CH ₃	1.67 (3H), s, 1.38 (3H), s

DMSO: Dimethyl sulfoxide

compartion with parent drug [23] and this is because the binding with B(OH)₂. The spectra of metalcomplexes (C₁-C₃) exhibited shifted to higher values in the chemical shift of C=O (β -lactam), C=O amide and CH-NH₂ and this is attributed to complexation with metal ions [23]. In (Mix.) spectrum, the carboxylic C=O band absent and appeared a new bands at δ 159.36, which assigned to δ C=N (imino group) [19].

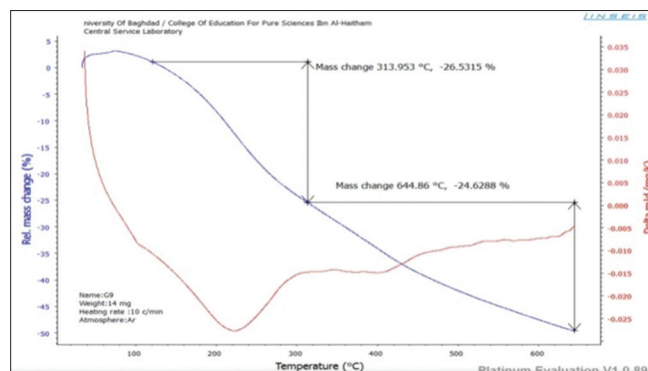


Fig. 2: The thermo gram of the Ligand

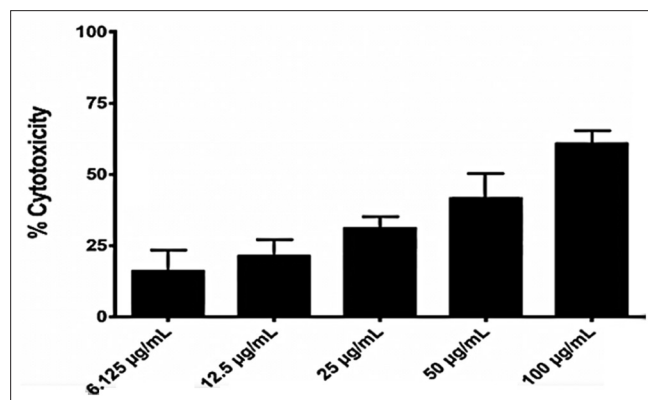
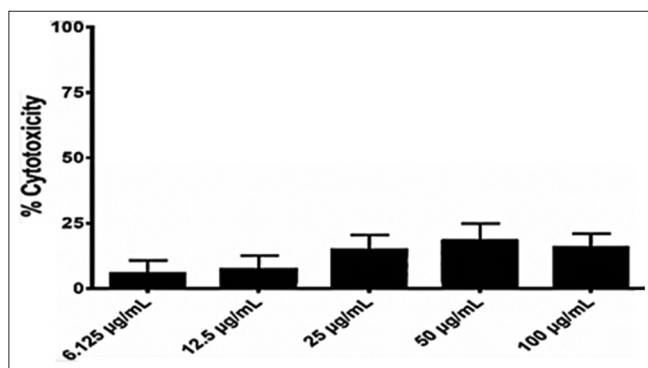
Fig. 3: Cytotoxic effect of (C₃) in AMJM

Fig. 4: Cytotoxic effect of (L) in SKOV-3

As well as the C=O (β -lactam), C=O (amide) and CH-NH₂ bands were shifted to higher values and this is because coordination with metal ions.

Electronic spectra

The electronic spectra of synthesized compounds were recorded in methanol (10^{-4} M) at room temperature. The spectral data were listed in Table 13. The electronic spectrum of ligand exhibited high intensity band in 356 nm (28089 cm^{-1}), which due to $\pi \rightarrow \pi^*$ transition [24]. In addition the spectrum of ligand showed low intensity bands at 373 nm (26809 cm^{-1}), which assigned to $n \rightarrow \pi^*$ transition [24]. The data were listed in Table 13. The spectrum of C_1 complex showed change in position of $\pi \rightarrow \pi^*$ transition (Table 14). The spectrum of C_1 complex exhibited two bands appeared at 585 nm (17049 cm^{-1}) and 805 nm (12422 cm^{-1}) which assigned to ${}^4T_1g \rightarrow {}^4T_1g$ (p) and ${}^4T_1g \rightarrow {}^4A_2g$ respectively [25]. The magnetic moment value of C_1 complex were found (Meff= 4.55 B.M) and this value is agreement with octahedral geometry [25]. The data were listed in Table 14. The spectrum of Ni (II) complex exhibited change in $\pi \rightarrow \pi^*$ transition. The spectrum of Ni (II) complex showed two bands at 610 nm (16393 cm^{-1}) and 951 nm (10515 cm^{-1}) which due to ${}^3A_2g \rightarrow {}^3T_1g$ (F) and ${}^3A_2g \rightarrow {}^3T_2g$ transition of octahedral Ni (II) complexes [25, 26]. The Meff of nickel C_2 were 3.42 B.M. This value agreement with octahedral

geometry [25-27]. The data were listed in Table 13. The spectra of copper complexes (C_3 and Mix.) complexes showed change in $\pi \rightarrow \pi^*$ transition (Table 14). The spectrum of C_3 complex showed three bands at 541 nm (18484 cm^{-1}), 651 nm (15360 cm^{-1}) and 761 nm (13140 cm^{-1}) which due to ${}^2B_1g \rightarrow {}^2Eg$, ${}^2B_1g \rightarrow {}^2B_2g$ and ${}^2B_1g \rightarrow {}^2A_1g$ transitions (Table 14) of distorted octahedral copper complexes [25] (Fig. 5). The spectrum of mixed ligand complex (Mix.) (Fig. 6) exhibited one

Table 6: 1HNMR data for C3

Assignments in d6-DMSO	Chemical shifts δ (ppm)
OH Phenolic	9.35 (1H), s
N-H Amide	9.08 (1H), s
B-OH	8.75 (1H), s
C-H aromatic	8.03–6.74 (4H), m
CHNH (β -lactam)	5.76 (1H), d
CHS (β -lactam)	5.35 (2H), s
NH ₂	5.20 (2H), s
CH-NH ₂	5.20 (1H), s
N-CH	3.94 (1H), s
H ₂ O	3.36 (4H), s
2CH ₃	1.55 (3H), s, 1.40 (3H), s

DMSO: Dimethyl sulfoxide

Table 7: 1HNMR data for mix

Assignments in d6-DMSO	Chemical shifts δ (ppm)
OH Phenolic	9.41 (1H), s
N-H Amide	9.04 (1H), s
B-OH	8.68 (2H), s
C-H aromatic	7.87–6.55 (9H), m
CHNH (β -lactam)	5.76 (1H), d
CHS (β -lactam)	5.36 (1H), d
NH ₂	5.29 (2H), s
CH-NH ₂	5.29 (1H), s
N-CH	4.32 (1H), s
H ₂ O	3.40 (4H), s
N-CH ₃	3.40 (3H), s
C-CH ₃	2.50 (3H), s
2CH ₃	1.63 (3H), s, 1.51 (3H), s

DMSO: Dimethyl sulfoxide

Table 8: 13CNMR data for the Ligand

Assignments in d6-DMSO	Chemical shifts δ (ppm)
COOB	173.36
C=O (β -lactam)	170.16
C=O (amide)	169.15
C (heterocyclic ring)	139.92
Aromatic carbon	130.30–112.80
CHNH (β -lactam)	61.17
CHS (β -lactam)	58.96
CH-NH ₂	57.84
C-S	26.51
2CH ₃	20.30, 18.15

Table 9: 13CNMR data for C1

Assignments in d6-DMSO	Chemical shifts δ (ppm)
C=O (β -lactam)	177.33
C=O (amide)	175.50
COOB	173.70
C (heterocyclic ring)	140.40
Aromatic carbon	130.24–113.38
CH-NH ₂	64.39
CHNH (β -lactam)	61.53
CHS (β -lactam)	59.39
C-S	25.51
2CH ₃	17.58, 16.35

Table 10: 13CNMR data for C2

Assignments in d6-DMSO	Chemical shifts δ (ppm)
C=O (β -lactam)	176.63
C=O (amide)	175.43
COOB	173.72
C (heterocyclic ring)	137.54
Aromatic carbon	133.55–115.18
CH-NH ₂	64.37
CHNH (β -lactam)	62.75
CHS (β -lactam)	58.50
C-S	26.82
2CH ₃	18.48, 15.83

Table 11: 13CNMR data for C3

Assignments in d6-DMSO	Chemical shifts δ (ppm)
C=O (β -lactam)	176.22
C=O (amide)	174.52
COOB	173.18
C (heterocyclic ring)	138.54
Aromatic carbon	132.84–112.13
CH-NH ₂	63.35
CHNH (β -lactam)	62.79
CHS (β -lactam)	58.53
C-S	26.88
2CH ₃	20.87, 18.18

Table 12: 13CNMR data for Mix

Assignments in d6-DMSO	Chemical shifts δ (ppm)
C=O (β -lactam)	176.71
C=O (amide)	175.35
C=N, C=O (4-aminoantipyrene)	159.36
C (heterocyclic ring)	140.43
C (4-aminoantipyrene)	134.54
Aromatic carbon	134.54–110.27
C-N (4-aminoantipyrene)	115.72
CH-NH ₂	66.31
C (β -lactam)	63.53
C (β -lactam)	57.94
N-CH ₃	39.08
C-S	23.57
2CH ₃	21.69, 18.37
CH ₃ (4-aminoantipyrene)	18.37

Table 13: Electronic transitions, molar conductivity, spectra, magnetic susceptibility and suggested geometry of the ligand and its metal complexes

Comp	Band positions nm (cm ⁻¹)	Assignment	Molar conductivity (S.cm ² .mol ⁻¹) in Methanol	μ _{eff.} (B.M)	Suggested geometry
L	356 (28089) 370 (27027)	(π→π*) (n→π*)	-----	-----	-----
C1	363 (27548) 585 (17094) 805 (12422)	(π→π*) ⁴ T _{1g} → ⁴ T _{1g} (P) ⁴ T _{1g} → ⁴ A _{2g}	25	4.55	Octahedral
C2	351 (28490) 610 (16393) 951 (10515)	(π→π*) ³ A _{2g} → ³ T _{1g} (F) ³ A _{2g} → ³ T _{2g}	23	3.42	Octahedral
C3	363 (27548) 541 (18484) 651 (15360) 761 (13140)	(π→π*) ² B _{1g} → ² E _g ² B _{1g} → ² B _{2g} ² B _{1g} → ² A _{1g}	30	1.96	distorted octahedral
Mix.	363 (27548) 758 (13192)	(π→π*) ² B _{1g} → ² A _{1g}	42	1.89	distorted octahedral

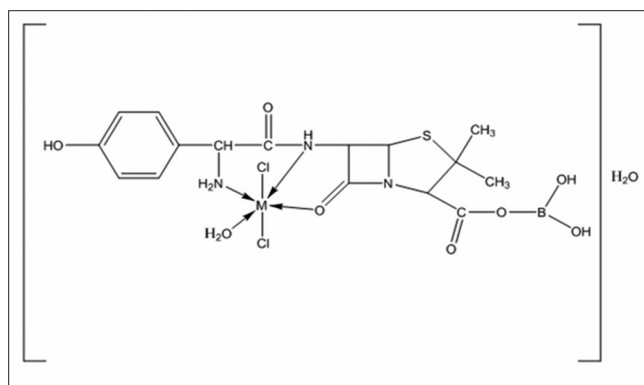
Table 14: Thermal decomposition data of the ligand (L) and its metal complexes

Molecular formula and Molecular weight	Step	Temp. rang of the Decomposition C°	DTG Temp C°	Suggested	Mass loss%
				Formula of loss	Cal. Found
C ₁₆ H ₂₀ N ₃ O ₇ SB 408.82	1	35-313.95	101, 225	H ₂ BO ₃ , 2CH ₃ , OH	26.36 26.53
	2	313.95-644.86	330, 375, 410, 517, 625	NH ₂ , SCCHCO	24.7 24.62
C ₁₆ H ₂₀ N ₃ O ₇ SBCo. 2Cl. 2H ₂ O 574.73	1	40-184.70	55, 100	HO (C ₆ H ₄) CHCONH (C ₃ H ₂ NO)	48.92 48.85
	2	184.70-272.07	235	2H ₂ O, OH	9.22 9.2
C ₁₆ H ₂₀ N ₃ O ₇ SB Ni. 2Cl. 2H ₂ O 574.49	3	272.07-642.59	300, 330, 450, 595, 625	2Cl, OH, CH ₃	17.92 17.9
	Residue	>650		(HO) C ₆ H ₄ CH (NH ₂) CO, CH ₃	28.71 28.83
C ₁₆ H ₂₀ N ₃ O ₇ SB Ni. 2Cl. 2H ₂ O 574.49	1	16-189.13	27, 50, 100, 120, 166	NHCH (CO) CH (N) SCCHCOOB Co	44.14 44.07
	2	189.13-259.07	227	H ₂ O	3.13 3.64
C ₁₆ H ₂₀ N ₃ O ₇ SBCu. 2Cl. 2H ₂ O 579.36	3	259.07-644.69	275, 318, 400, 475, 558, 583, 633	H ₂ O, 2Cl	15.49 15.96
	Residue	>650		SC (CH ₃) ₂ CHCOOB (OH) ₂	30.6 30.83
C ₁₆ H ₂₀ N ₃ O ₇ SBCu. 2Cl. 2H ₂ O 579.36	1	25-258.56	45, 85, 100	HO (C ₆ H ₄) CH (NH ₂)	50.77 49.57
	2	125.56-384.19	230, 280	CONH (C ₃ H ₂ NO) Ni	13.94 13.92
C ₂₇ H ₃₁ N ₆ O ₆ SB Cu. 2Cl. 2H ₂ O 764.36	3	384.19-644.61	440, 465, 520, 590, 635	2H ₂ O, H ₂ BO ₃	22.61 22.59
	Residue	>650		2Cl, NH ₂ , CO ₂	12.42 12.2
C ₂₇ H ₃₁ N ₆ O ₆ SB Cu. 2Cl. 2H ₂ O 764.36	1	25-161.83	40, 75, 100, 120	C (CH ₃) ₂ CH, OH	51.01 51.29
	2	161.83-230.82	187	(C ₆ H ₄) CHCONHCH (CO) CH (S)	11.51 11.53
C ₂₇ H ₃₁ N ₆ O ₆ SB Cu. 2Cl. 2H ₂ O 764.36	3	230.82-360.37	285, 345	(N) Cu	8.63 7.95
	4	360.37-494.13	405, 457	2H ₂ O, 2CH ₃	11.51 11.53
C ₂₇ H ₃₁ N ₆ O ₆ SB Cu. 2Cl. 2H ₂ O 764.36	5	494.13-643.86	535, 570, 610	2Cl, OH	11.51 11.53
	Residue	>650		C=C (CH ₃) N (CH ₃) N (C ₆ H ₅) CO, SC, 2OH	34.66 34.97
C ₂₇ H ₃₁ N ₆ O ₆ SB Cu. 2Cl. 2H ₂ O 764.36	1	25-161.83	40, 75, 100, 120	(C ₆ H ₄) CHNH ₂	13.73 13.61
	2	161.83-230.82	187	CONHCHCHNCHC (N) OB	19.46 19.31
C ₂₇ H ₃₁ N ₆ O ₆ SB Cu. 2Cl. 2H ₂ O 764.36	3	230.82-360.37	285, 345	COCu	11.98 12.63
	4	360.37-494.13	405, 457		
C ₂₇ H ₃₁ N ₆ O ₆ SB Cu. 2Cl. 2H ₂ O 764.36	5	494.13-643.86	535, 570, 610		
	Residue	>650			

Table 15: The biological activity for compounds in 10⁻² and 10⁻³ M

Compound	<i>P. auroginosa</i>		<i>S. aureus</i>		<i>E. coli</i>	
	Inhibition zone diameter (mm)					
	10 ⁻²	10 ⁻³	10 ⁻²	10 ⁻³	10 ⁻²	10 ⁻³
DMSO	-	-	-	-	-	-
Amoxicillin	-	14	14	-	15	15
Boric acid	-	-	12	14	-	-
L	-	-	14	12	-	11
C1	11	-	15	11	11	13
C2	13	-	14	11	13	11
C3	19	10	28	12	18	18
Mix.	17	7	30	11	17	17

E. coli: *Escherichia coli*, *P. auroginosa*: *Pseudomonas auroginosa*

**Fig. 5: Structure of the complex (C₁, C₂ and C₃)**

band at 758 nm (13192 cm⁻¹), this band due to ²B_{1g}→²A_{1g} transition of distorted octahedral Cu (II) complex [25] (Fig. 7). The magnetic moment of copper complexes were 1.96 and 1.89 B.M of C₃ and

Mix. respectively, these values of Meff agreement with distorted octahedral geometry [25]. All complexes exhibited a nonelectrolyte behavior [28] (Table 13).

Thermal analysis of the ligand and its metal complexes

The TG and DTG analysis were performed under nitrogen gas in the range heating 16–650°C and the heating rate (10°C/min). This technique was used to study the thermal stability of synthesized compounds as well as to characterize the suggested structures. The thermal decomposition data were listed in (Table 14) and the thermographs of the ligand (L) and C_1 complex were shown in (Figs. 2 and 8). The results showed that the stability of the ligand and its complexes was increase as the following order Mix. $<C_1 < L_1 < C_2 < C_3$. The results of degradation exhibited good agreement in percentage of calculate and found mass loss and this confirm the suggested structures of synthesized compounds [29].

Biological activity

The antibacterial activity of the ligand (L) and its metal complexes have been evaluated against (*P. auroginosa*, *E. coli* (G-) and

Staphylococcus aureus (G+)). The bacterial activity was test with two concentration (10^{-2} and 10^{-3} M) of the primary materials and all synthesized compounds. The C_3 and Mix. in 10^{-2} M were the most effective against the studied microorganism. The ligand (L) exhibited small activity with *S. aureus* comparison with its complexes. All synthesized compounds in 10^{-3} M were more active from the parint drug against *S. aureus*. The antibacterial data were listed in (Table 15). DMSO solvent was used as control [30].

Hepatoprotective and kidney evaluation

Hepatoprotective evaluations included assessment of liver function enzyme (GOT, GPT and ALP) and renal function test (Urea, Creatinine, TSP and Alb) in serum. The results were listed in (Tables 16 and 17). The obtained results showed the positive effect of all studied compound on GOT, GPT, ALP, Urea, Creatinine, TSP and Alb.

Histopathological evaluation

The results of histopathological evaluation of liver and kidney tissue which treated with C_3 and Mix. showed the positive effect

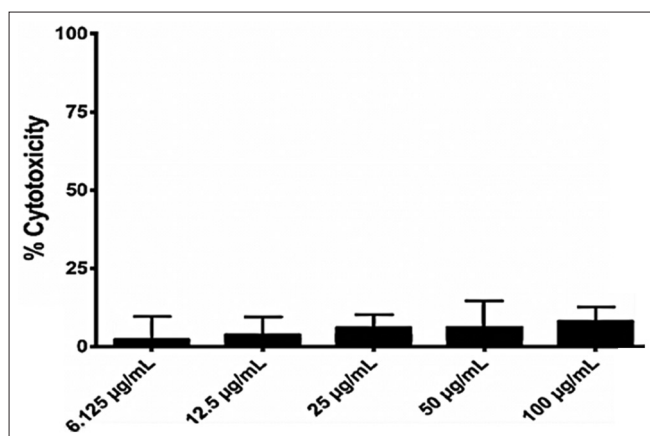


Fig. 6: Cytotoxic effect of (L) in CMF-7

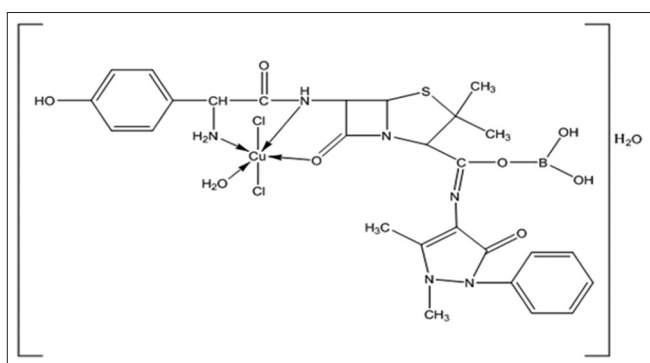


Fig. 7: Structure of the complex (Mix.) M= Co (II), Ni (II) and Cu (II)

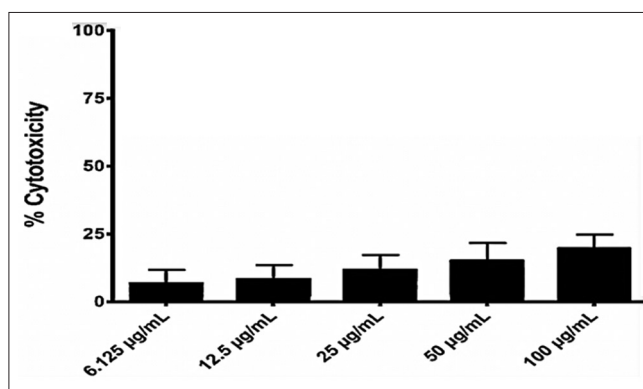


Fig. 9: Cytotoxic effect of ligand (L) in AMJM

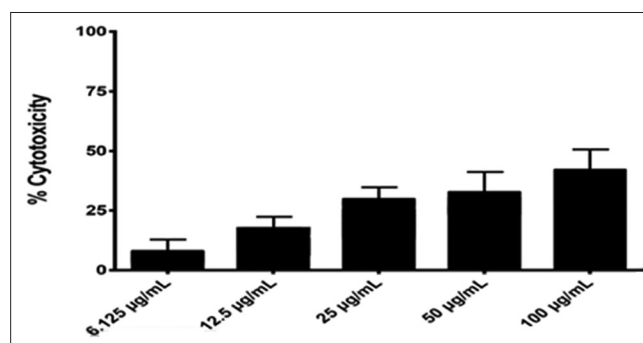


Fig. 10: Cytotoxic effect of (C_3) in SKOV-3

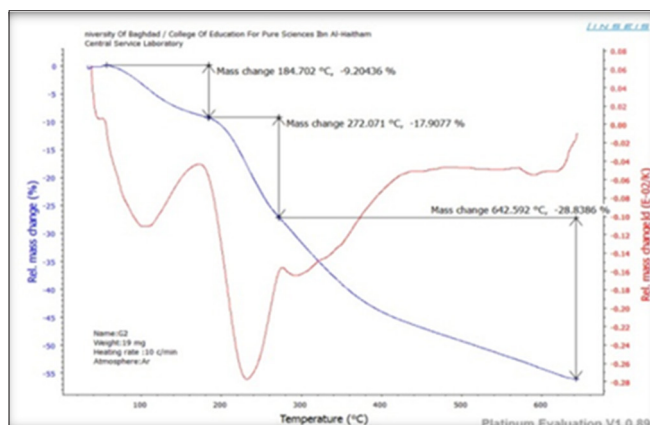


Fig. 8: The thermogram of the cobalt complex (C_1)

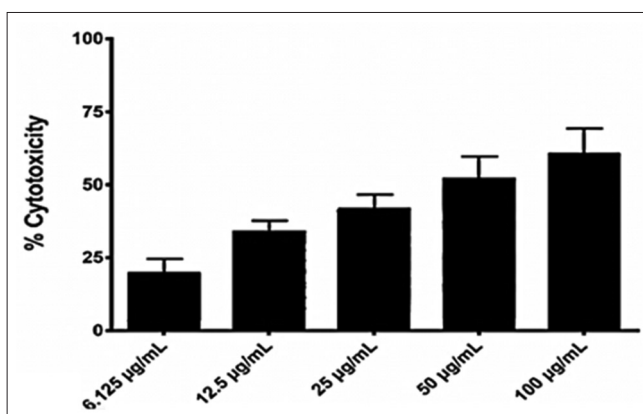


Fig. 11: Cytotoxic effect of (Mix.) in CMF-7

of studied compounds and no negative effect were on tissue observed.

Anticancer activity (cytotoxicity assays)

Study of anticancer activity for amoxicillin, L, C₃ and Mix. was carried out on different cancer cell lines (AMJM, SOK-7 and CMF-3). The inhibition rate of cell growth (the percentage of cytotoxicity) was calculated as the following equation:

$$\text{Inhibition rate} = \frac{A-B}{A} \times 100$$

Where A and B are the optical density of control and the optical density of test.

The study of anticancer activity for the ligand exhibited high percentage of cytotoxicity comparison with amoxicillin, this is due to presence of

boron element and this is agreement with literature [31]. The increase in percentage of cell inhibition due to presence of β -lactam ring in all studied compounds as well as presence of aromatic ring in Mix. (4-Aminoantipyrine) and this is enhanced the anticancer activity [32]. Also found that the Schiff base ligand improve the anticancer activity [33]. The Schiff base linkage ($-C=N$) is an essential structural requirement for antitumor activities [33, 34]. Cytotoxicity assays of ligand and its complexes are shown in Tables 18-20 and Figs. 9-11 for L and C₃.

DPPH radical scavenging activity (RSA) (antioxidant activity)

2,2-diphenyl-1-picryl-hydrazyl (DPPH) was used in RSA for the evaluation of antioxidant and this is the rapid technique for screening the RSA of specific compounds or extracts [35]. DPPH is a stable free radical that can accept an electron or hydrogen radical and get converted to a stable, diamagnetic molecule. The results of this study showed that the ligand exhibited a negligible DPPH activity. In

Table 16: Effect of the Ligand (L) and its metal complexes on liver function enzymes (GOT, GPT and ALP) in sera of albino male mice

Groups	Dose (mg/Kg)	GOT (Mean+Standard error of mean)	GPT (Mean+Standard error of mean)	ALP (Mean+Standard error of mean)
Control	0.625	38.50±0.50	50.50±2.50	64.00±4.00
L	0.625	21.00±1.00	35.50±1.50	49.00±3.00
C3	0.625	27.50±0.50	50.00±2.50	84.50±4.50
Mix.	0.625	42.00±1.50	58.90±4.00	90.50±3.50

GOT: Glutamic oxaloacetic transaminase, GPT: Glutamate pyruvate transaminase, ALP: Alkaline phosphatase

Table 17: Effect of the Ligand (L) and its Metal Complexes on Renal Function Test (Urea, Creatinine, Alb and TSP) in Sera of Albino Male Mice

Groups	Dose (mg/Kg)	Urea (Mean±Standard error of mean)	Creatinine (Mean±Standard error of mean)	Alb (Mean±Standard error of mean)	Total protein (Mean±Standard error of mean)
Control	0.625	31.55±1.45	0.55±0.045	3.05±0.15	7.65±0.35
L	0.625	42.70±2.70	0.31±0.01	2.80±0.10	7.95±0.35
C3	0.625	32.70±0.10	0.085±0.005	3.00±0.10	8.05±0.05
Mix.	0.625	33.95±1.25	0.065±0.005	2.95±0.05	8.40±0.50

Alb: Albumin, TSP: Total serum protein

Table 18: Cytotoxicity Assays (AMJM) Cell of the Ligand and its Metal Complexes

Comp.	Conc. (6.125 µg/mL)	Conc. (12.5 µg/L)	Conc. (25 µg/mL)	Conc. (50 µg/m)	Conc. (100 µg/L)
Cytotoxicity%					
Amoxicillin	2.78	4.16	4.16	4.16	2.78
L	6.67	8.33	13.33	18.33	23.33
C3	16.18	20.59	32.35	44.12	61.77
Mix.	16.07	32.04	48.08	49.84	65.86

Table 19: Cytotoxicity Assays (SKOV-3) Cell of the Ligand and its Metal Complexes

Comp.	Conc. (6.125 µg/L)	Conc. (12.5 µg/L)	Conc. (25 µg/mL)	Conc. (50 µg/mL)	Conc. (100 µg/mL)
Cytotoxicity%					
Amoxicillin	2.70	2.08	4.16	2.71	5.55
L	6.67	8.33	13.33	18.33	23.33
C3	7.69	17.30	29.34	32.69	42.30
Mix.	7.81	9.33	15.92	26.56	32.81

Table 20: Cytotoxicity assays (MCF-7) cell of the ligand and its metal complexes

Comp.	Conc. (6.125 µg/L)	Conc. (12.5 µg/L)	Conc. (25 µg/mL)	Conc. (50 µg/mL)	Conc. (100 µg/L)
Cytotoxicity%					
Amoxicillin	3.12	2.34	4.68	3.12	5.46
L	2.63	3.94	6.57	6.57	8.54
C3	16.70	21.71	25.05	21.70	25.05
Mix.	20.00	34.15	42.25	53.44	61.79

Table 21: DPPH RSA for the ligand and its metal complexes with comparison ascorbic acid

Comp.	Conc. (25 µg/mL)	Conc. (50 µg/mL)	Ascorbic acid
% Scavenging activity			
L	30	46	78
C1	30	56.25	85
C2	33.33	40	73.33
C3	40	71.11	91.10
Mix.	37.78	62.22	77.78

RSA: Radical scavenging activity

complexes, the results showed that the scavenging activity % of C3 and Mix. (Cu (II) complexes) were more than the free ligand and this is due to presence of Cu (II) ion [36], while the other complexes exhibited different scavenging activity. (Table 21)

CONCLUSION

New compound was synthesized by the insertion of boron on amoxicillin, also some metal complexes of this ligand were synthesized as well as we are synthesized the mixed ligand (copper complex with ligand and 4-aminoantipyrine) was synthesized. All compounds were characterized by different techniques. The antibacterial activities for all compounds were evaluation. The results showed that copper complexes were more active in (10^{-2} M) than the other compounds. The ligand (L) exhibited small activity with *S. aureus* comparison with its complexes, All synthesized compounds in 10^{-3} M were more active from the amoxicillin against *S. aureus*. The medicinal studies were performed on the ligand and its metal complexes such as study the effect of synthesized compounds on the liver and kidney enzymes. The positive result were observed and the studied compounds improvement the activity of enzymes. Also the studies showed the positive results on the normal liver and kidney tissues. Another studies (anticancer and antioxidant activity) were carried out and the results were encouraging to use as anticancer and antioxidant agents.

AUTHORS' CONTRIBUTION

All authors have contributed equally.

CONFLICTS OF INTEREST

Authors have no conflicts of interest.

REFERENCES

- Kistler RB, Helvacı. C. Boron and borates. *Ind Miner Rocks* 1994;6:171-86.
- Dieter MP. Toxicity and carcinogenicity studies of boric acid in male and female B6C3F1 mice. *Environ Health Perspect* 1994;102 Suppl 7:93-7.
- Karimi-Maleh H, Tahernejad-Javazmi F, Gupta VK, Ahmar H, Asadi MH. A novel biosensor for liquid phase determination of glutathione and amoxicillin in biological and pharmaceutical samples using a ZnO/CNTs nanocomposite/ catechol derivative modified electrode. *J Mol Liq* 2014;196:258-63.
- Refat MS, Al-Maydama HM, Al-Azab FM, Amin RR, Jamil YM. Synthesis, thermal and spectroscopic behaviors of metal-drug complexes: La(III), Ce(III), Sm(III) and Y(III) amoxicillin trihydrate antibiotic drug complexes. *Spectrochim Acta A Mol Biomol Spectrosc* 2014;128:427-46.
- Li Y, Liu Y, Wang H, Xiong X, Wei P, Li F, *et al.* Synthesis, crystal structure, vibration spectral, and DFT studies of 4-aminoantipyrine and its derivatives. *Molecules* 2013;18:877-93.
- Reitman S, Frankel S. A colorimetric method for the determination of serum glutamic oxalacetic and glutamic pyruvic transaminases. *Am J Clin Pathol* 1957;28:56-63.
- Gometi SA, OguguaVN, Odo CE, Joshua PE. Effects of some anti-diabetic plants on the hepatic marker enzymes of diabetic rats. *Afr J Biotechnol* 2014;13:905-9.
- Kuan JC, Lau KY, Guilbault GG. Enzymatic determination of serum urea on the surface of silicone-rubber pads. *Clin Chem* 1975;21:67-70.
- Artiss JD, McEnroe RJ, Zak B. Bilirubin interference in a peroxidase-coupled procedure for creatinine eliminated by bilirubin oxidase. *Clin Chem* 1984;30:1389-92.
- Wayner DD, Burton GW, Ingold KU, Locke S. Quantitative measurement of the total, peroxy radical-trapping antioxidant capability of human blood plasma by controlled peroxidation. The important contribution made by plasma proteins. *FEBS Lett* 1985;187:33-7.
- Pérez-Serrano J, Denegri G, Casado N, Rodríguez-Caabeiro F. *In vivo* effect of oral albendazole and albendazole sulphoxide on development of secondary echinococcosis in mice. *Int J Parasitol* 1997;27:1341-5.
- Fu W, Chen J, Cai Y, Lei Y, Chen L, Pei L, *et al.* Antioxidant, free radical scavenging, anti-inflammatory and hepatoprotective potential of the extract from *Parathelypteris nipponica* (Franch. Et sav.) ching. *J Ethnopharmacol* 2010;130:521-8.
- Al-Shammari AM, Salman MI, Saihood YD, Yaseen NY, Raed K, Shaker HK, *et al.* *In vitro* synergistic enhancement of newcastle disease virus to 5-fluorouracil cytotoxicity against tumor cells. *Biomedicines* 2016;4:E3.
- Sulaiman GM, Jabir MS, Hameed AH. Nanoscale modification of chrysin for improved of therapeutic efficiency and cytotoxicity. *Artif Cells Nanomed Biotechnol* 2018;46:708-20.
- Al-Noor TH, Jarad AJ, Hussein AO. Synthetic, spectroscopic and antibacterial studies of Fe (II), Co (II), Ni (II), Cu (II), Zn (II), Cd (II) and Hg (II), mixed ligand complexes of saccharin and amoxicillin (antibiotics). *Chem Mater Res* 2014;6:20-30.
- Piskin S, Yilmaz MS. Production of Methyl Borate for Sodium Borohydride (NaBH₄): Hydrogen Storage Medium. Bangkok: In: International Conference on Chemistry and Chemical Process; 2011.
- Ansari RM, Bhat BR. Schiff base transition metal complexes for suzuki miyaura cross-coupling reaction. *J Chem Sci* 2017;129:1483-90.
- Mohammed AM, Salim JS. Synthesis and biological evaluation of new boron compound with cephalixin and some of its transition metal complexes. *J Glob Pharm Technol* 2018;10:640-9.
- Spinu C, Kriza A. Co (II), Ni (II) and Cu (II) complexes of bidentate Schiff bases. *Acta Chim Slov* 2000;47:179-86.
- Tomı IH, Abdullah AH, Al-Daraji AH, Abbas SA. Synthesis, characterization and comparative study the antibacterial activities of some imine-amoxicillin derivatives. *Eur J Chem* 2013;4:153-6.
- Martin C, Ronda J, Cadiz V. Boron-containing novolac resins as flame retardant materials. *Polym Degrad Stab* 2006;91:747-54.
- Mohammed A. Synthesis and biological evaluation of new boron compound with cephalixin and some of its transition metal complexes. *J Glob Pharm Technol* 2018;10:640-9.
- Fleming I, Williams DH. *Spectroscopic Methods in Organic Chemistry*. London: McGraw-Hill; 1966.
- Al-Abidy N. Synthesis, Characterization and Study of the Biological Activity of New Mannich-Schiff Bases and Some Metal Complexes Derived from Isatin, 3-Amino-1, 2, 4-Triazol and Dithiooxamide. Iraq: University of Baghdad Baghdad; 2006.
- Al-Jeboori FH, Al-Shimiesawi TA, Oun MA, Abd-ul-Ridha A, Abdulla AY. Synthesis and characterization of amino acid (phenylalanine) schiff bases and their metal complexes. *J Chem Pharma Res* 2014;6:44-53.
- Figgis BN. *Introduction to Ligand Fields*. New York: Interscience Publishers; 1966.
- Geary WJ. The use of conductivity measurements in organic solvents for the characterisation of coordination compounds. *Coord Chem Rev* 1971;7:81-122.
- Badea M, Olar R, Uivarosı V, Marinescu D, Aldea V, Barbuceanu SF, *et al.* Thermal behavior of some vanadyl complexes with flavone derivatives as potential insulin-mimetic agents. *J Therm Anal Calorim* 2011;105:559-64.
- Scorei RI, Popa R Jr. Boron-containing compounds as preventive and chemotherapeutic agents for cancer. *Anticancer Agents Med Chem* 2010;10:346-51.
- Rajput R, Mishra AP. A review on biological activity of quinazolinones. *Int J Pharm Sci* 2012;4:66-70.
- Banik I, Becker FF, Banik BK. Stereoselective synthesis of beta-lactams with polyaromatic imines: Entry to new and novel anticancer agents. *J Med Chem* 2003;46:12-5.
- Creaven BS, Duff B, Egan DA, Kavanagh K, Rosair G, Thangella VR, *et al.* Anticancer and antifungal activity of Copper (II) complexes of quinolin-2 (1H)-one-derived Schiff bases. *Inorganica Chim Acta* 2010;363:4048-58.
- Verlee A, Mincke S, Stevens CV. Recent developments in antibacterial and antifungal chitosan and its derivatives. *Carbohydr Polym* 2017;164:268-83.
- Prakash CR, Raja S, Saravanan G. Synthesis, characterization and anticonvulsant activity of novel Schiff base of isatin derivatives. *Int J*

- Pharm Sci 2010;2:177-81.
35. Amarowicz R, Pegg R, Rahimi-Moghaddam P, Barl B, Weil J. Free-radical scavenging capacity and antioxidant activity of selected plant species from the Canadian prairies. *Food Chem* 2004;84:551-62.
 36. Barik A, Mishra B, Shen L, Mohan H, Kadam RM, Dutta S, *et al.* Evaluation of a new Copper(II)-curcumin complex as superoxide dismutase mimic and its free radical reactions. *Free Radic Biol Med* 2005;39:811-22.